

## DETERMINATION OF DUCTILITY CAPACITY AND OTHER SECTION PROPERTIES OF T-SHAPED RC WALLS IN DIRECT DISPLACEMENT-BASED DESIGN

E. Smyrou<sup>1</sup>, T.J. Sullivan<sup>2</sup>, M.J.N. Priestley<sup>3</sup> and G.M. Calvi<sup>4</sup>

<sup>1</sup> *PhD Candidate, Centre of Research and Graduate Studies in Earthquake Engineering and Engineering Seismology (Rose School), Pavia, Italy*

<sup>2</sup> *Assistant Professor, Dept. of Structural Mechanics, University of Pavia, Pavia, Italy*

<sup>3</sup> *Professor, Centre of Research and Graduate Studies in Earthquake Engineering and Engineering Seismology (Rose School), Pavia, Italy*

<sup>4</sup> *Professor, Centre of Research and Graduate Studies in Earthquake Engineering and Engineering Seismology (Rose School) & Dept. of Structural Mechanics, University of Pavia, Pavia, Italy  
Email: smiroulena@gmail.com*

### ABSTRACT :

In this paper, the behaviour of T-shaped walls is determined by examining the relative effect of the web-flange ratio, the reinforcement percentage and the axial load on curvature through the employment extensive moment-curvature analyses. T-shaped walls of different web-flange ratio with varying axial load, reinforcement content and distribution within a representative range of values are analysed in order to determine the curvature trends for three limit states, i.e. serviceability, yield and ultimate. A comprehensive set of equations for yield, serviceability and ultimate curvature is proposed, indicating the level of uncertainty for each expression. The proposed expressions, being adapted to different levels of precision and accompanied by graphical representation, lead to the reliable computation of limit-state curvatures, essential within a displacement-based design approach, and can be utilised in the realistic estimation of appropriate ductility factors in the design of T-shaped walls. Furthermore, the results regarding the section properties of T-shaped walls, such as the elastic stiffness and the moment capacity for opposite directions of loading, offer additional information useful in the design of T-shaped walls.

**KEYWORDS:** T-shaped walls, direct displacement-based design, limit-state curvatures, section properties

### 1. INTRODUCTION

In current design it is commonly assumed that the stiffness is a fundamental property of a RC section, implying that the yield curvature is directly proportional to the yield moment. However, extensive analyses on several types of sections, the strength of which was altered by changing the axial load or the flexural reinforcement content, have shown that the stiffness and strength vary essentially in proportion (Priestley, 1993). Finding that the stiffness and strength are independent for a given structural member type and size, it follows that the curvature, and consequently the member displacement, is independent and thus an important parameter in the stiffness calculations. However, until now the sections examined regarding walls were mostly rectangular, although in reality for both structural and architectural purposes walls rarely follow this configuration, exhibiting several shapes. One of the most commonly used types of walls is the T-shaped walls, the behaviour of which differs significantly from that of rectangular walls in terms of stiffness, strength and ductility capacity, strongly depending on the direction of the loading, as will be shown in this work.

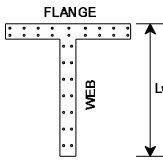
## 2. ANALYSES RESULTS

### 2.1. Considerations in Moment-Curvature Analyses

In this work, T-shaped RC walls with different ratio of flange width over web length are considered. This ratio will be called web-flange ratio henceforth. Moment-curvature analyses were conducted (XTRACT, 2004) for all the sections with varying axial load ratio and longitudinal reinforcement ratio in order to determine trends in the moment-curvature relationships of the T-shaped walls for yield curvature, as well as for the curvatures at serviceability and damage control limit states. Specifically, the ratios of flange width over web of the sections analyzed are presented in Table 1. The thickness of the web and flange was considered equal to 250mm, with two layers of reinforcing confining an inner core.

Table 1 Dimensions of T-shaped walls examined

Web Length (m)	Flange Width (m)				
6.0	4.0	3.0	2.0	1.5	1.0
4.0	4.0				
3.0	4.0				
2.0	4.0				



The ratio of longitudinal reinforcement, defined as  $\rho = A_s/A_g$ , took the values of 0.005, 0.010, 0.015 and 0.020 for the case of uniform distribution of the reinforcement, the advantages of such a configuration are advocated by Priestley et al. (2007). Moreover, the case of concentrated reinforcement at the ends of the sections was examined. In particular, 0.5% of the reinforcement was distributed along the web, while the rest was concentrated at the ends of the web and flange, in such a way that the reinforcement at the web end did not exceed 4% of the wall end area. Consequently, the  $\rho$  ratios considered were 0.010, 0.015 and 0.020. The axial load ratio, i.e.  $N/f_c A_g$ , varied between zero and 0.10.

Finally, as far as the material properties are concerned, the concrete compressive strength is taken equal to 30MPa, while the steel yield strength is 450MPa. The effects of steel strain hardening and concrete confinement were considered and the confined concrete was differentiated from the unconfined. In the analyses conducted, the Mander concrete model (1988) was used. The reinforcement is inserted as discrete. It is noted that the doubly-reinforced wall sections are regarded well-designed with sufficient confinement that deters the buckling of the compressive rebars.

### 2.2. Definition of Limit-State Curvatures

Yield curvature  $\phi_y$  was defined as the curvature found by extrapolating the line from the origin of the moment-curvature curve through first yield ( $M_y, \phi'_y$ ) to the nominal strength  $M_N$ . The first yield occurs for the lower of the curvatures corresponding to  $\epsilon_s = \epsilon_y$  for steel and  $\epsilon_c = 0.002$  for concrete. The nominal moment is defined as the one at curvature corresponding either to  $\epsilon_s = 0.015$  or  $\epsilon_c = 0.004$ , whichever happens first. This latter curvature is in fact the serviceability curvature  $\phi_s$ . The values of strains for the serviceability curvature correspond to the onset of incipient spalling for concrete, and for steel strains that result in residual crack widths greater than 1.0mm. Finally, the damage control or ultimate curvature  $\phi_u$  is defined as the lower of the curvatures corresponding to  $\epsilon_s = 0.060$  and  $\epsilon_c = 0.018$ , which are estimates of damage-control limit strains for well-confined concrete and well-restrained reinforcement. The limit to confined concrete compression strain is based on when fracture of transverse reinforcement occurs. Further discussion on the derivation or the conservatism of these strain values can be found in Priestley and Kowalsky (1998).

### 2.3. Graphical Representation of Limit-State Curvatures

Considering the amount of moment-curvature results, obtained for the many different T-shaped walls with different properties in each direction of loading, there is need of an effective way of

representation. However, this representation is rendered complicated due to the involvement of four parameters, i.e. web-flange ratio, axial load, reinforcement percentage and of course dimensionless curvature. Therefore, Figure 1 to 3 were produced, relating the different percentages of reinforcement with their contours presenting the values of dimensionless curvature in relation to the axial and web-flange ratio, given respectively in the horizontal and vertical axis, offering an immediate comparison of the values of dimensionless curvature. Due to limited space, the equivalent graphs for concentrated reinforcement are not presented in this paper, but can be found in Smyrou (2008).

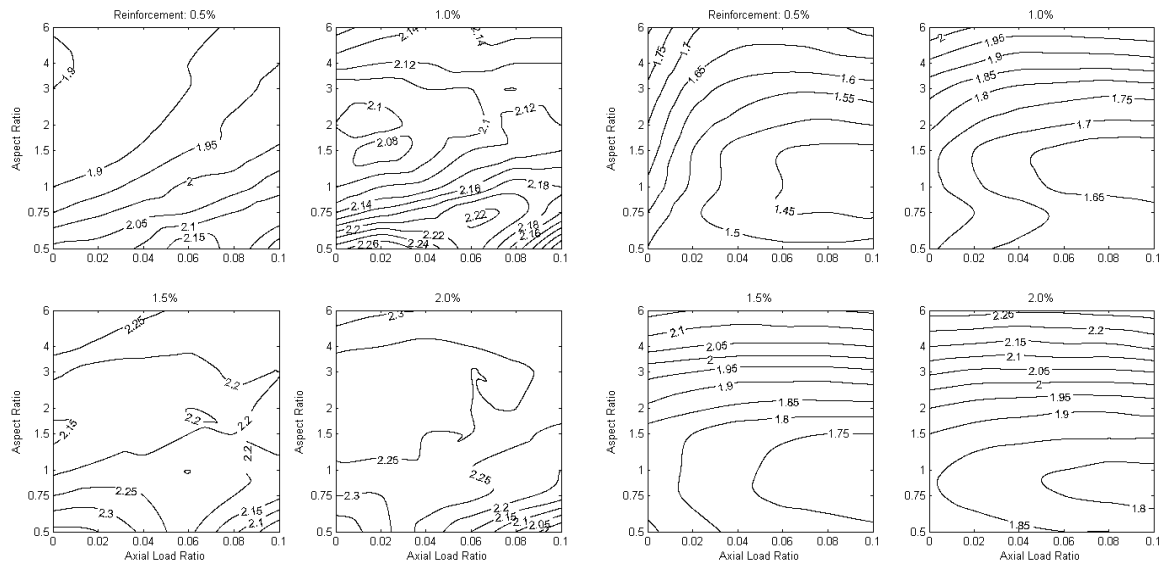


Figure 1 Dimensionless yield curvature  $K_y$  for flange in tension (left) and compression (right) for uniform distribution of reinforcement

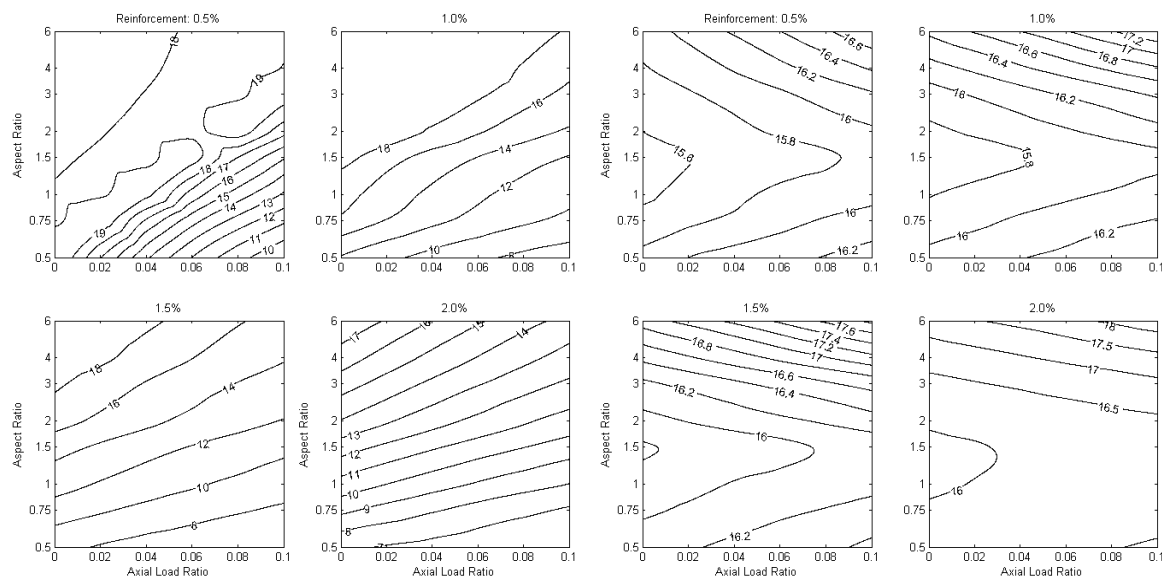


Figure 2 Dimensionless serviceability curvature  $K_s$  for flange in tension (left) and compression (right) for uniform distribution of reinforcement

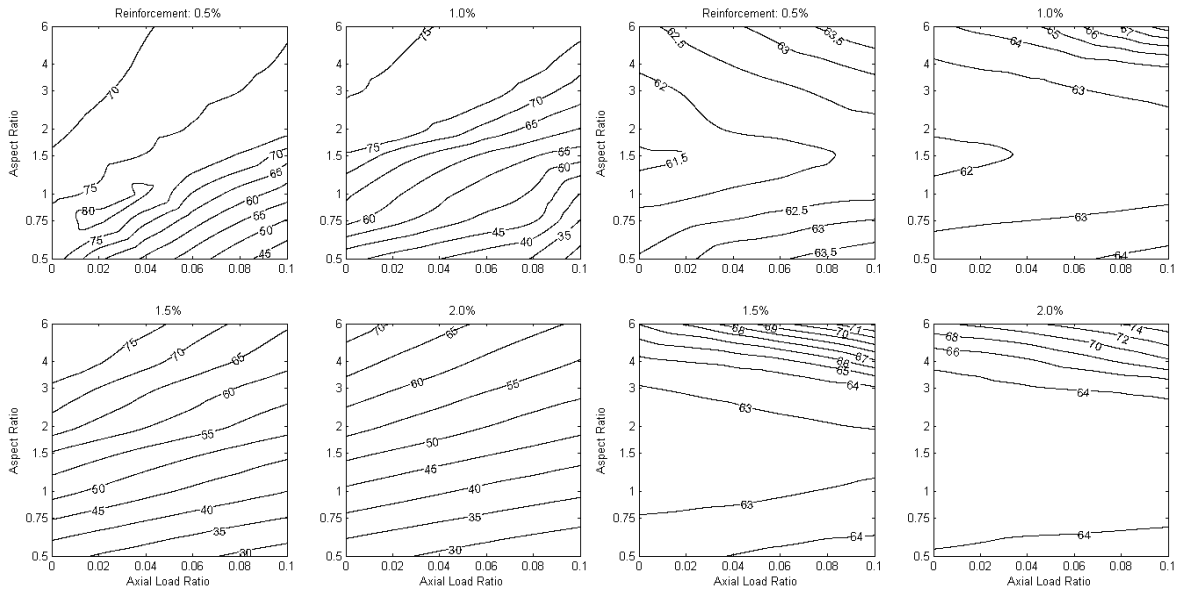


Figure 3 Dimensionless damage-control curvature  $K_u$  for flange in tension (left) and compression (right) for uniform distribution of reinforcement

#### 2.4. Analytical Representation of Limit-State Curvatures

Evaluating the variation in the results of the moment-curvature analyses, it is inferred that the dimensionless curvature can be expressed by a set of equations. The expressions proposed will be different for flange in tension (FiT) and in compression (FiC), as well as for uniformly distributed and concentrated reinforcement. The equations given in the following sections were obtained after regression analysis, where all the moment-curvature analyses results were considered and special effort was made in order to minimise the variation.

##### 2.4.1 Yield curvature

The expressions proposed for the dimensionless yield curvature follow the general form:

$$K_y = \kappa + xA + y \cdot (\rho - \lambda) \pm \% \quad (2.1)$$

where  $A$  is the web-flange ratio and  $\rho$  is the reinforcement content. The yield curvature can be expressed in a general form as  $\phi_y = K_y \cdot \epsilon_y / l_w$  (Paulay, 2002). The constants, best-fit for the equations, vary for flange in tension and compression, as well as for distributed and concentrated reinforcement (Table 2).

Table 2 Parameters for yield curvature expression including  $\rho$

	Uniform reinforcement		Concentrated reinforcement	
	FiT	FiC	FiT	FiC
$x$	-0.008	0.045	0.005	0.07
$y$	-0.8	20	10	20
$\kappa$	2.15	1.80	2.10	2.00
$\lambda$	-0.05	0.02	0.015	0.036
$\%$	12	9	9	8

Proceeding with simplifying the previous expressions, the reinforcement ratio is removed as variable

from the equations proposed, still leading to satisfactory percentage of variation. The simplified expressions have the same form, though they do not include the same constant term. The exclusive participation of the web-flange ratio renders the detection of the effect of the geometry of the section easy. Note that in the case of flange in tension for uniform distribution of reinforcement the effect of  $A$  is insignificant, so it can be eliminated. The expressions including only  $A$  follow the form:

$$K_y = x + yA \pm \% \quad (2.2)$$

Table 3 Parameters for yield curvature expression including only  $A$

	Uniform reinforcement		Concentrated reinforcement	
	FiT	FiC	FiT	FiC
x	2.15	1.57	2.15	1.60
y	0	0.06	-0.023	0.06
%	13	16	10	14

Alternatively, the expression suggested can be reduced to simpler ones, different for each case, that take a constant form. This simplification requires a compromise in the precision in the case of flange in compression, since it leads to higher percentage of variation. Specifically, for the uniformly distributed reinforcement the expressions respectively for flange in tension and compression are:

$$\phi_{y,FiT} = 2.15 \cdot \varepsilon_y / l_w \pm 13\% \quad (2.3)$$

$$\phi_{y,FiC} = 1.75 \cdot \varepsilon_y / l_w \pm 23\% \quad (2.4)$$

For concentrated reinforcement the equivalent expressions are:

$$\phi_{y,FiT} = 2.15 \cdot \varepsilon_y / l_w \pm 12\% \quad (2.5)$$

$$\phi_{y,FiC} = 1.80 \cdot \varepsilon_y / l_w \pm 20\% \quad (2.6)$$

The aforementioned relations offer in a simple way a good estimate of the yield curvature. In fact they can be reduced in one regardless of the reinforcement configuration, where the dimensionless yield curvature  $K$  takes the values 2.15 and 1.80 for flange in tension and compression respectively.

#### 2.4.2 Serviceability curvature

In the case of the serviceability curvature for flange in tension, it is rather difficult to fix a representative expression. The obtained relation takes a sophisticated form and exhibits significantly high variation. The general form of the relation for flange in tension is given by Eqn. 2.7, while the parameters involved are presented in Table 4.

$$K_{s,FiT} = 16 - xp - (N/\rho)^y + zA \pm \% \quad (2.7)$$

Table 4 Parameters for serviceability curvature expression

	Uniform reinforcement	Concentrated reinforcement
	FiT	FiT
x	400	300
y	0.5	0.6
z	1.3	1.5
%	35	35

It is reminded that  $A$  is the web-flange ratio,  $\rho$  is the reinforcement ratio and  $N$  is the axial load ratio, which has an effect on the serviceability curvature and therefore is included. Finally, it is underlined that the values corresponding to flange in tension should be treated cautiously and are given for the sake of completeness with doubts about their usefulness.

On the contrary, for flange in compression a low variation makes possible the use an expression for the serviceability curvature of a constant form. Therefore, the expression for the flange in compression has constant form and coincides for both uniform and concentrated reinforcement, with 9% and 12% percentage of variation respectively. Specifically:

$$K_{s, FiC} = 17 \pm \% \quad (2.8)$$

It is reminded that  $\phi_s = K_s / 1000 \cdot l_w$ . Since the limit curvatures for serviceability, proposed by Priestley and Kowalsky (1998) for rectangular walls, are directly related to maximum permissible tension strains, it is expected that they can be applied with reasonable accuracy to flanged wall sections such as T-shaped ones, provided that the flange is in compression, while for flange in tension lower values should be used (Priestley et al., 2007). This statement is confirmed by the findings of this work, since the derived expression of the serviceability curvature when flange is in compression differs slightly from the equivalent by Priestley and Kowalsky (1998), according to whom the predicted value for  $K_s$  is equal to 17.5. Moreover, the values obtained by the more complex expression for serviceability curvature, when flange is in tension, tend to the value for rectangular walls, especially when the reinforcement is higher and the flange width decreases, approaching thus the shape of rectangular wall. For the other T-shaped walls, lower values are achieved for flange in tension.

#### 2.4.3 Damage-control curvature

Similar conclusions found for the serviceability curvature are drawn for the damage control curvature. The expressions obtained for flange in tension are characterised by complexity and very high variability, rendering them thus hard to use and unreliable for the estimation of the ultimate curvature for flange in tension. Therefore, it is judged that there is little point in presenting them. The variables involved (web-flange ratio, axial load ratio, reinforcement ratio) are in such a way inter-correlated that no specific trend for the ultimate curvature for flange in tension can be identified. Indicatively, it is mentioned that the values of  $K_u$  for flange in tension and web-flange ratio greater than 1.0 range between 40 and 80. Hence, the readers are referred to Smyrou (2008) for the exact values, as well as to Figure 3. On the other hand, in the case of flange in compression the ultimate curvature can be estimate with absolute precision, something expected by the shape of the relative curves. That is why no percentage of variation is given for the respective relations. The expressions for flange in compression for uniform and concentrated reinforcement are respectively given by Eqn. 2.9 and 2.10. It is characteristic that the damage control curvature depends exclusively on the web-flange ratio.

$$K_{u, FiC} = 65 + 0.5A \quad (2.9)$$

$$K_{u, FiT} = 65 + 1.1A \quad (2.10)$$

The reader is reminded that these expressions have been developed for web-flange ratios between 0.5 and 6.0. As previously, note that  $\phi_u = K_u / 1000 \cdot l_w$ .

#### 2.5. Moment Capacity of T-Shaped Sections

The results from the full set of moment-curvature analyses provided data for the nominal moment capacity of the T-shaped walls, which is of interest considering the asymmetry of the T-shaped sections. The dimensionless nominal moment  $M_{DN}$  is defined as

$$M_{DN} = M_N / f_y \cdot t \cdot l_w^2 \quad (2.11)$$

where  $M_N$  is the nominal moment,  $f_y$  is the yield strength of steel,  $l_w$  is the web length and  $t$  is the web width. Note that for both FiT and FiC, the web width is used in the expression of  $M_{DN}$ , as the comparison becomes easier by having a common definition. Traditionally, dimensionless moment capacity has been related to concrete compression strength, rather than the steel yield strength, but the moments, for the axial load ratios relevant to walls are almost independent of concrete strength, and directly proportional to steel yield strength (Priestley et al., 2007). The dimensionless results are expected to apply to other wall section sizes and material strengths within the normal range of material strengths.

Indicatively, the graphs of dimensionless moment for both directions of loading for solely one web-flange ratio are provided in Figure 4. Due to space limitations, the complete set of relative graphs is not shown but can be found in the work by Smyrou (2008). As expected, the dimensionless moment reduces with decreasing reinforcement ratio. The difference in the moment capacity of the two directions becomes more pronounced as the web-flange ratio decreases, since the presence of a strong flange contributes significantly to the moment capacity of the section. This difference is less intense for concentrated reinforcement, because the reinforcement at the web tip improves the moment capacity of the relatively weaker web. The moment capacity for flange in tension is constantly higher than the moment for flange in compression, with the exception of sections with concentrated reinforcement and high web-flange ratio, in which the flange-in-compression moment is comparable or slightly exceeds the equivalent for flange in tension.

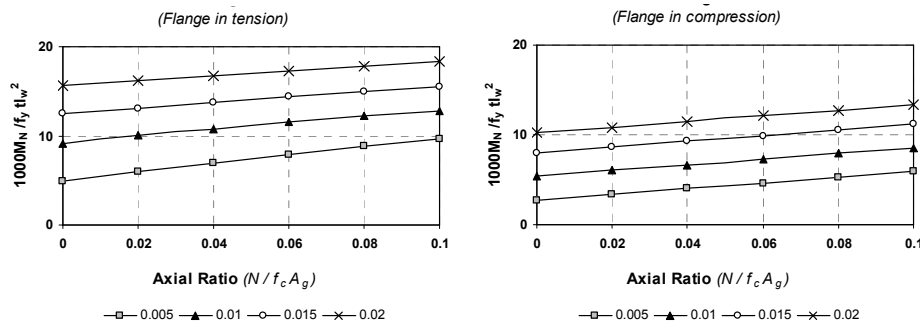


Figure 4 Dimensionless moment for web-flange ratio 2.0 (uniformly distributed reinforcement)

### 2.5. Elastic Stiffness of T-Shaped Sections

The elastic stiffness of the T-shaped walls, defined by the nominal moment  $M_N$  and the yield curvature  $\phi_y$ , to the initial uncracked section stiffness  $EI_{gross}$  is given by

$$\frac{EI}{EI_{gross}} = \frac{M_N}{\phi_y EI_{gross}} \quad (2.12)$$

It is noted that the stiffness of the gross uncracked section was computed ignoring the stiffening effect of flexural reinforcement. As expected, the elastic stiffness increases for increasing reinforcement amount and axial load ratio, with the former being notably more influential. In particular, in case of the uniformly distributed reinforcement and for web-flange ratios less than unity, the elastic stiffness is approximately double of the equivalent for flange in compression, reflecting the dominance of the flange's presence. For web-flange ratios higher than unity the values of elastic stiffness for both directions of loading are comparable but those for flange in tension remain higher, something that becomes less evident for decreasing flange width. For concentrated reinforcement the elastic stiffness values in general are relatively augmented. For web-flange ratios higher than unity, the flange-in-compression elastic stiffness is interestingly higher than the corresponding one for flange in

tension, which is exclusively attributed to the concentrated amount of reinforcement at the web tip that manages to outbalance the effect of the flange. This is not achieved for web-flange ratios less than unity, in which the flange still dominates. However, by concentrating the reinforcement the characteristic of T-shaped sections difference in stiffness can be cancelled, which can prove useful in design. In general, depending on the web-flange ratio and the reinforcement configuration, the elastic stiffness in any of the two directions of loading for T-shaped walls can deviate substantially from the values reported for the elastic stiffness of rectangular walls (Priestley et al., 2007). Moreover, the fact that the range of elastic stiffness varies quite significantly underlines the strong dependence of elastic stiffness on axial load ratio and reinforcement ratio. Clearly, the common assumption of constant section stiffness independent of flexural strength is entirely inappropriate. As previously, a sample of graphs of the elastic stiffness of T-shaped sections is given in Figure 5.

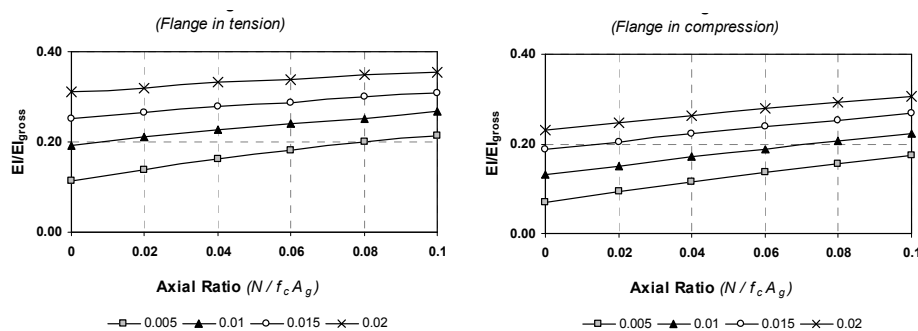


Figure 5 Elastic stiffness for web-flange ratio 2.0 (uniformly distributed reinforcement)

### 3. CONCLUSIONS

Curvature relationships for the yield, serviceability and damage-control curvatures were developed for T-shaped walls with regard to their asymmetric properties. The results were presented by graphical and analytical means as a function of axial load ratio and reinforcement content for different levels of complexity. Thus, the estimation of appropriate curvature ductility factors for each limit-state can be realised. In conjunction with the information on the moment capacity and the elastic stiffness provided, the properties of T-shaped sections are completely and realistically defined and constitute useful and necessary tool for Direct Displacement-Based Design of T-shaped RC walls.

### REFERENCES

- Mander, J.P., Priestley, M.J.N. and Park, R. (1988). Theoretical stress-strain model for confined concrete. *Journal Structural Engineering ASCE* **114:8**, 1804-1826.
- Priestley, M.J.N., Calvi, G.M. and Kowalsky, M.J. (2007). Displacement-based seismic design of structures, IUSS press, Pavia, Italy.
- Priestley M.J.N. and Kowalsky, M.J. (1998). Aspects of drift and ductility capacity of cantilever structural walls. *Bulletin of New Zealand National Society for Earthquake Engineering* **31:2**, 73-85.
- Priestley, M.J.N. (1993). Myths and fallacies in earthquake engineering – Conflicts between design and reality. *Bulletin of New Zealand National Society for Earthquake Engineering* **26:3**, 329-341.
- Smyrou, E. (2008). Seismic design of T-shaped RC walls, PhD Thesis, Rose School, IUSS press, Pavia, Italy (in preparation).
- XTRACT (2004). Cross sectional X sTRuctural Analysis of ComponenTs, Imbsen Software Systems.
- Paulay, T. (2002). An estimation of displacement limits for ductile systems. *Earthquake Engineering and Structural Dynamics*, **31**, 583–599.

**The 14<sup>th</sup> World Conference on Earthquake Engineering  
October 12-17, 2008, Beijing, China**

